Phase Equilibria in the System KASH
$(K_2O - Al_2O_3 - SiO_2 - H_2O)$

Jomaah A. Alawi

Department of Geology, College of Science, King Saud University,
P.O. Box 2455, Riyadh 11451, Saudi Arabia

Abstract. Six solid phases, Diaspore, Microcline, Quartz, Pyrophyllite, Kaolinite, and Muscovite were chosen to construct a P-T grid for the system KASH ($K_2O - Al_2O_3 - SiO_2 - H_2O$). This 4-component 7-phase multisystem contains 6 invariant points and 15 univariant curves, which, when connected, generate a unique P-T net. Using thermodynamic data, topology, and graphical analysis according to the Schreinemaker's rule, ten P-T nets of maximum closure were constructed. Based on the signs and magnitudes of entropies, molar volumes, and slopes associated with the univariant reactions, the nets are oriented with respect to temperature and pressure coordinates. Only one net, namely ((K) (M)) is suitable to represent the phase relations in the system. The use of different thermodynamic data changes the net orientation and to some extent yields fairly different results. This puts some doubt on the reliability of thermodynamic data as criteria for selecting from the possible diagrams and on the validity of the chosen P-T net. A program (SUPCRT) was run at different P and T conditions for the reaction (diaspore + 2 quartz = pyrophyllite + water). The information was used to determine P and T of equilibrium and to evaluate the sign and magnitude of the slope of the univariant line in order to confirm the reliability of the proposed net orientation. The results show a very steep positive slope and equilibrium T = 312°C at P = 2.5 Kbar. A chemical potential ($\mu K_2O - \mu SiO_2$) diagram constructed by using different thermodynamic sources also emphasizes how the error factor in thermodynamic data affects the interpretation of phase diagrams.

Application to natural geologic occurrences, especially to metapelites and pyrophyllite deposits, indicates that the phase diagram obtained may define mineralogical relations and chemical equilibria in natural processes.

Introduction

The quaternary system KASH ($K_2O - Al_2O_3 - SiO_2 - H_2O$) includes a considerable number of minerals which form under a wide range of temperature (T) and pressure (P) conditions. The most common minerals and species in the system are corundum,

Jomaah A. Alawi

potassium oxide and hydroxide, silicon oxides (which include nine polymorphs), water, aluminium hydrates (diaspore, boehmite, and gibbsite), aluminium silicates (andalusite, kyanite, sillimanite and mullite), clay minerals (kaolinite, dickite, nacrite, and halloysite), pyrophyllite, kalsilite, leucite, potassium feldspar (microcline, orthoclase, adularia, and sanidine), and muscovite. If a buffered chemical potential of water is assumed, that is if $\mu\ H_2O$ is held constant (fixed water activity due to the presence of water as a distinct phase of fixed composition in the system), then the above mineral assemblages can be represented on a triangular composition diagram in the system KASH (Fig. 1).
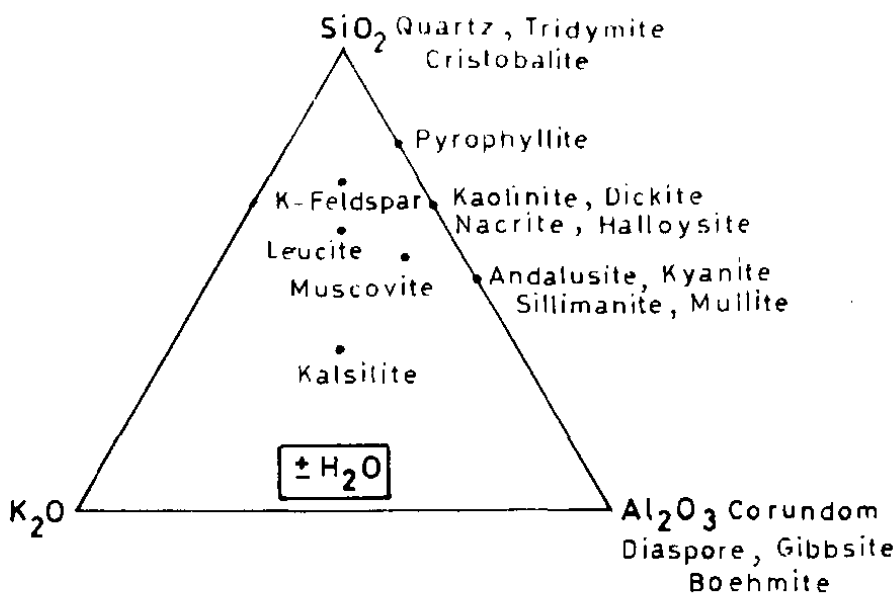

Fig. 1. Triangular composition diagram in the system KASH $(K_2O - Al_2O_3 - SiO_2 - H_2O)$, $\mu\ H_2O$ is held constant.

In this work, six solid phases have been chosen (Table 1) and arranged in a triangular diagram to show the chemographic relations under different conditions (Fig. 2). Using thermodynamic data, both under high and low P and T and using graphical and topological analyses following the Schreinemaker's rule, the stability relations of the different mineral phases in P-T space are determined. A P-T net representative of the system can then be constructed and oriented. This net may, therefore, be used to describe the conditions of formation of certain low T and P natural assemblages pertinent to the studied system.

Degeneracy

The chemical potential of H_2O is suggested to be buffered to the system due to the presence of water as a distinct phase (Fig. 2). The system can be represented as

Table 1. Symbols and chemical formulae of the six solid phases selected to represent the system KASH on a P.T. diagram.

Phases and Phase Number	Symbols	Chemical Formulae	Oxide Formulae
Diaspore (1)	D	$AlO(OH) \times 2$	$1\,Al_2O_3 \cdot 1 \cdot H_2O$
Microcline (2)	F	$KAlSi_3O_8 \times 2$	$1\,K_2O \cdot 1\,Al_2O_3 \cdot 6SiO_2$
Quartz (3)	Q	SiO_2	$1\,SiO_2$
Pyrophyllite (4)	P	$Al_2Si_4O_{10}(OH)$	$1\,Al_2O_3 \cdot 4SiO_2 \cdot 1H_2O$
Kaolinite (5)	K	$Al_2Si_2O_5(OH)$	$1\,Al_2O_3 \cdot 2SiO_2 \cdot 2H_2O$
Muscovite (6)	M	$KAl_2(AlSi_3O_{10}(OH_2) \times 2$	$1\,K_2O \cdot 3Al_2O_3 \cdot 6SiO_2 \cdot 2H_2O$
Water (7)	W	H_2O	$1\,H_2O$
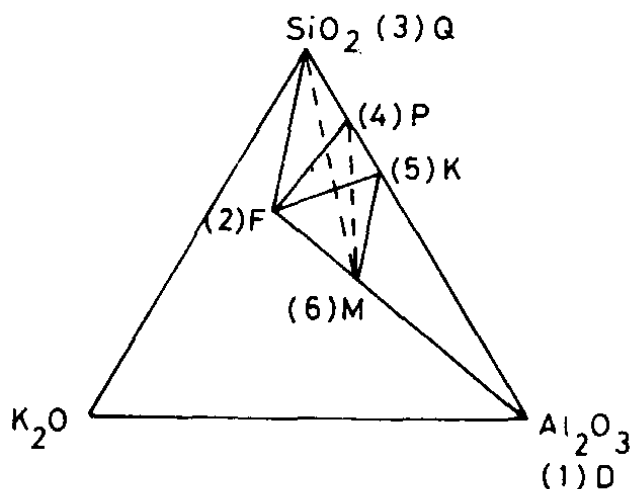
Fig. 2. Triangular composition diagram showing the chemographic relations of the selected six solid phases in the system KASH, with H_2O buffered to the system. The dashed tie-line indicates a metastable relation while the solid line represents stable equilibrium. By convention a phase is represented as a filled circle.

pseudo ternary and the diagram reveals that the system is degenerate, that is, containing two different sets of degenerate relations that occur simultaneously. First, one compositional collinearity of three phases in which the singular phases are F,M and D whereas the other three phases K, P and Q are indifferent. Second, one compositional collinearity of four phases in which the singular phases are D,K,P and Q while phases F and M are indifferent. It should be noted that polymorphism, such as the silicon oxide polymorphs, aluminium hydrates and silicates, and clay mineral polymorphs, has largely contributed to the general degeneracy of the system.

Temperature-Pressure Grids in the System KASH

System topology

To set up the general outline for the construction of a P-T net, first a set of six P-T diagrams are drawn, each containing one invariant point and five univariant lines (curves). The diagrams are constructed based on the geometric method, (Shreinemaker's method) of representing heterogenous phase equilibria [1]. The data on the entropies and molar volumes (Table 2, from [2]) were used to determine the slopes of the curves using the Clapeyron Equation and to orient properly the univariant curves with respect to both temperature and pressure axes on a P-T diagram.

Table 2. Entropy of formation and molar volume of minerals and related species at 298.15° K and 1.0 bar pressure: (1) from [2] and (2) from [20].

Chemical Species	S (cal/deg) (1)	V (cal/bar) (1)	S (cal/deg) (2)	V (cal/bar) (2)
Alumina	12.17	0.611257	12.18	0.611257
Potash	22.50	0.965105	22.50	0.965105
Water	16.72	0.431860	16.71	0.431860
Diaspore	8.43	0.424470	8.43	0.424470
Microcline	51.20	2.598470	51.13	2.598948
Quartz	9.95	0.542260	9.88	0.542260
Pyrophyllite	57.220	3.054970	57.20	3.025813
Kaolinite	48.530	2.378590	48.53	2.378590
Muscovite	73.230	3.363050	68.80	3.363050

The univariant and divariant equilibria are designated in this paper according to Schreinemaker's notation, that is, by giving the phase or phases that do not participate in the reactions (absent phases) in parentheses. The number of phase labels appearing within a given parenthesis indicates the variance of the equilibrium [1].

In the system $K_2O - Al_2O_3 - SiO_2$ (3-component system), the number of the univariant reactions is reduced because of degeneracy, and the system can be completely discribed by a combination of eight reactions (Table 3). A set of six P-T diagrams can be constructed and properly oriented using the data from Table 2.

The six P-T diagrams mentioned above may be combined into a partially closed net/residual net drawn and oriented with respect to both T and P coordinates.

The direction of increasing T and P is shown by arrows which point toward the assemblages of higher entropies (bold arrows) and lower volume (broken arrows)

Table 3. Calculated entropy and volume changes of reactions and slopes (dp/dt = S/V) of univariant lines: (1) from [2] and (2) from [20].

Univariant Lines	Univariant Reactions	S Cal/deg (1)	V Cal/bar (1)	dp/dt bar/deg (1)	S Cal/deg (2)	V Cal/bar (2)	dp/dt bar/deg (2)
(D,Q)	M + P + 2W = 2K + F	− 15.63	+ 0.0740	− 211.22	− 11.23	+ 0.07440	− 150.95
(D,P)	M + 2Q + W = K + F	− 10.12	+ 0.0980	− 103.27	− 5.61	+ 0.09811	− 57.18
(D,K)	M + 4Q = P + F	− 4.61	+ 0.1214	− 37.97	+ 5.01	+ 0.09269	+ 0.108
(D,F,M)	K + 2Q = P + W	+ 5.51	+ 0.0240	+ 229.58	+ 5.62	− 0.00662	− 848.69
(Q,F,M)	2D + P + 2W = 2K	− 10.46	− 0.0105	+ 996.20	− 10.42	+ 0.01869	− 557.52
(P,F,M)	2D + 2Q + W = K	− 4.95	+ 0.0133	− 372.20	− 4.80	+ 0.01088	− 441.18
(P,Q,K)	2D + F = M	+ 5.17	− 0.0850	− 60.82	+ 4.80	− 0.07840	− 10.33
(K,F,M)	2D + 4Q = P	+ 0.56	− 0.0370	+ 15.14	+ 0.82	+ 0.00785	+ 104.46

respectively. The use of arrow systems to orient the closed regions in P-T space was first advocated by Zen [1].

Partially closed P-T net of maximum closure

In a multisystem of n-components, where n + 3 = number of solid phases, the different invariant equilibrium systems are separated from one another by univarant and divariant equilibrium systems. For a given set of chemographic relations among the n + 3 phases the univariant lines are the permissible consistent passageways among invariant assemblages which constitute a net of univariant lines linking invariant points on a P-T diagram.

In the system KASH the degeneracy common to the system reduces the univariant relations to only eight degenerate reactions (Table 3). The procedure to derive the closed net for both degenerate or non-degenerate chemographies is discussed before [3-7]. For the KASH, the possible chemography of the six solid phases is triangular with two simultaneous types of degeneracy (Fig. 2). It corresponds exactly to the ternary degenerate chemography T 49 of [4] as shown labelled in Fig. 3. Therefore, the permissible net topologies may be represented by Fig. 4 (a triangle with a central invariant point) and Fig. 5 (a square) and there are ten possible nets labelled as follows:

Fig. 4: ((4) (2)), ((3) (5)), ((5) (6)), ((4) (5)), and ((2) (6))
Fig. 5: ((4) (2)), ((3) (5)), ((5) (6)), ((4) (5)), and ((2) (6))

The numbers in parentheses indicate the phases that do not participate in the construction of the closed net (metastable phases) and could be replaced by letter labels according to Table 1. Schematic illustrations of the possible P-T nets of maximum closure, drawn according to Schreinemaker's rule are shown in Fig. 6.

Orientation of the P-T Nets

In order to determine which of the nets obtained most closely represents the phase equilibrium relations in the studied system, thermodynamic data are used. Entropy changes (Δ S) and volume changes (Δ V) of the eight degenerate reactions are given (Table 3) from two different sources. Using Δ S, arrows are drawn across the univariant lines pointing toward the high entropy assemblages favoured by increasing T, that is, to the direction in which univariant reactions result in an increase of T (and Entropy). For any closed portion of the diagram, the arrows must point both inward and outward (inside and outside the region). If the arrows point either all inward or all outward, then it is topologically impossible to orient that closed region in a T space, and the net cannot be oriented with respect to the T axis. The volume change can be used in the same manner. In this case, the arrows must
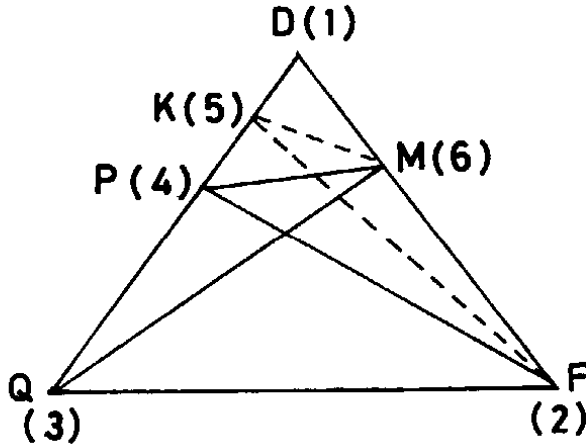
Fig. 3. Ternary degenerate chemography for the system KASH corresponding to T 49 of [4].
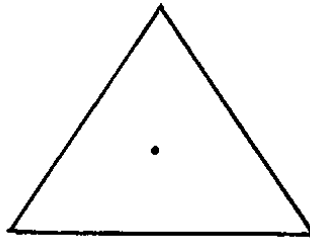
Fig. 4. First permissible net topology in the degenerate chemography of the system KASH (a triangle with a central invariant point).
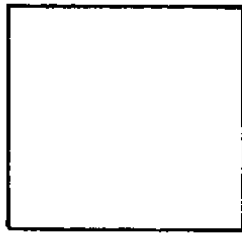
Fig. 5. Second permissible net topology in the degenerate chemography of the system KASH (a square without invariant point in the center).

point toward the low volume assemblages which must be formed under high P. Estimates of V are believed to be more reliable than estimates of S and the pressure directions are most suitable for net orientation [4]. However, P and T criteria are complementary in order that a hypothetical net be representative of the real phase relations in the studied equilibria.

Fig. 6. Set of seven nets of maximum closure oriented according to thermodynamic data of Table 3(2). The elimination of a net on the basis of P and/or T arrows is indicated by (P), (T), or (P & T) beneath each net.

Discussion

Temperature and pressure arrows have been drawn for all the nets of Fig. 6 using the data of Table 3(1). Six of these nets were eliminated on the basis of P (Fig. 6a), T (Fig. 6d, e, and f), or P & T (Fig. 6b and c) arrows. Only the arrows on Fig. 6g are compatible with the orientation rela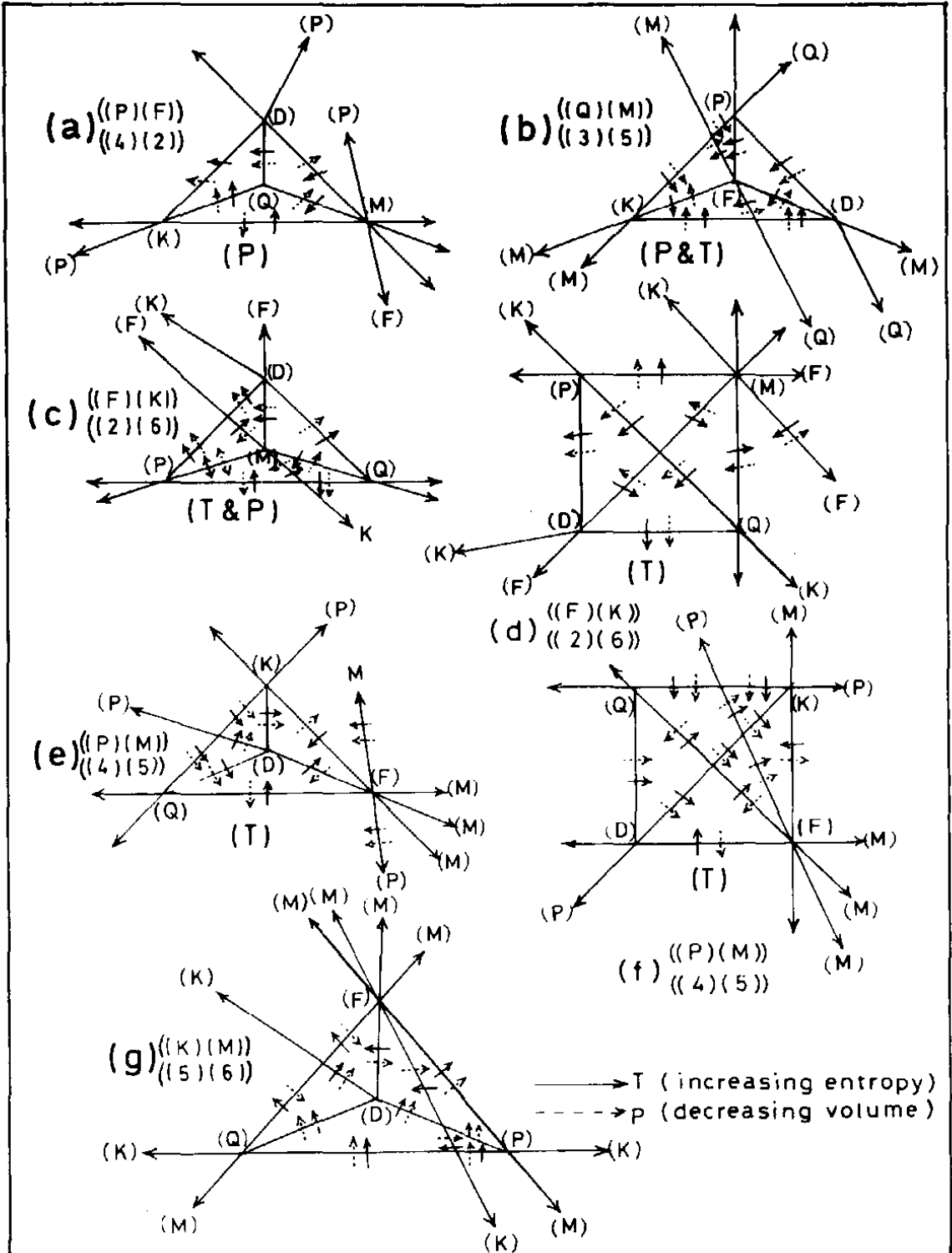tive to both P and T axes. The net ((K) (M)) is, therefore, the most suitable for further investigation in the system KASH.

It is worth pointing out that using the data of Table 3(2) yields somewhat different results. For instance, the $\triangle$ S of reaction (D,K) becomes slightly positive and the slope of the univariant line (D,K) also becomes positive. For reaction (D,F,M) the $\triangle$ V becomes negative and the slope becomes negative too, and for reaction (Q,F,M) the $\triangle$ V becomes positive and the slope becomes negative. These variations in the results put some doubt on the reliability of thermodynamic data as criteria for choosing from the different nets. Also, note that with appropriate changes in some of the $\triangle$ S or $\triangle$ V data of Table 3, any particular net can readily be oriented with respect to both T and P axes. For example, the net ((P) (F)), Fig. 6a, can be oriented in both P and T spaces povided $\triangle$ V of reaction (K,F,M) becomes slightly negative. Also the net ((P) (M)) can be oriented with respect to both axes if $\triangle$ S of reaction (K,F,M) changes from + 0.56 cal to slightly negative. This number (+ 0.56 cal) is less than the uncertainity in $\triangle$ S (Entropy of Formation) of any phase involved in the reaction. The fact that use of different sets of thermodynamic data gives different dP/dT values and thus does not yield the same P-T diagrams is a problem which is extensively discussed. Several authors [8-15] have studies such inconsistencies and emphasized the role of data uncertainty in causing discrepancies.

Using the slopes of the univariant curves the final topology of the oriented, partially closed net of maximum closure in the system KASH is illustrated in Fig. 7. Fortunately, the difference in the results of calculated $\triangle$ S and $\triangle$ V does not greatly affect the orientation scheme of the net ((K) (M)). However, changes in the slope values and slight shifts in the location of high and low P and T assemblages are observed.

Modification of the Grid in View of Experimental and Petrographic Data

The reaction 2 D + 4 Q = P represents the univariant line (K,F,M) which emanates from the invariant point (F) with a positive slope (Fig. 7). As shown on the grid diaspore and quartz are the low T-high P assemblage and pyrophyllite is the low P-high T assemblage. The entropy associated with the above reaction is very small (Table 3) and the error associated with the reported entropy values at 298.15° K and 1.0 bar pressure permits diaspore and quartz to be stable at high T. This change in the stability fields would have little effect on the previous orientation of the net ((K)
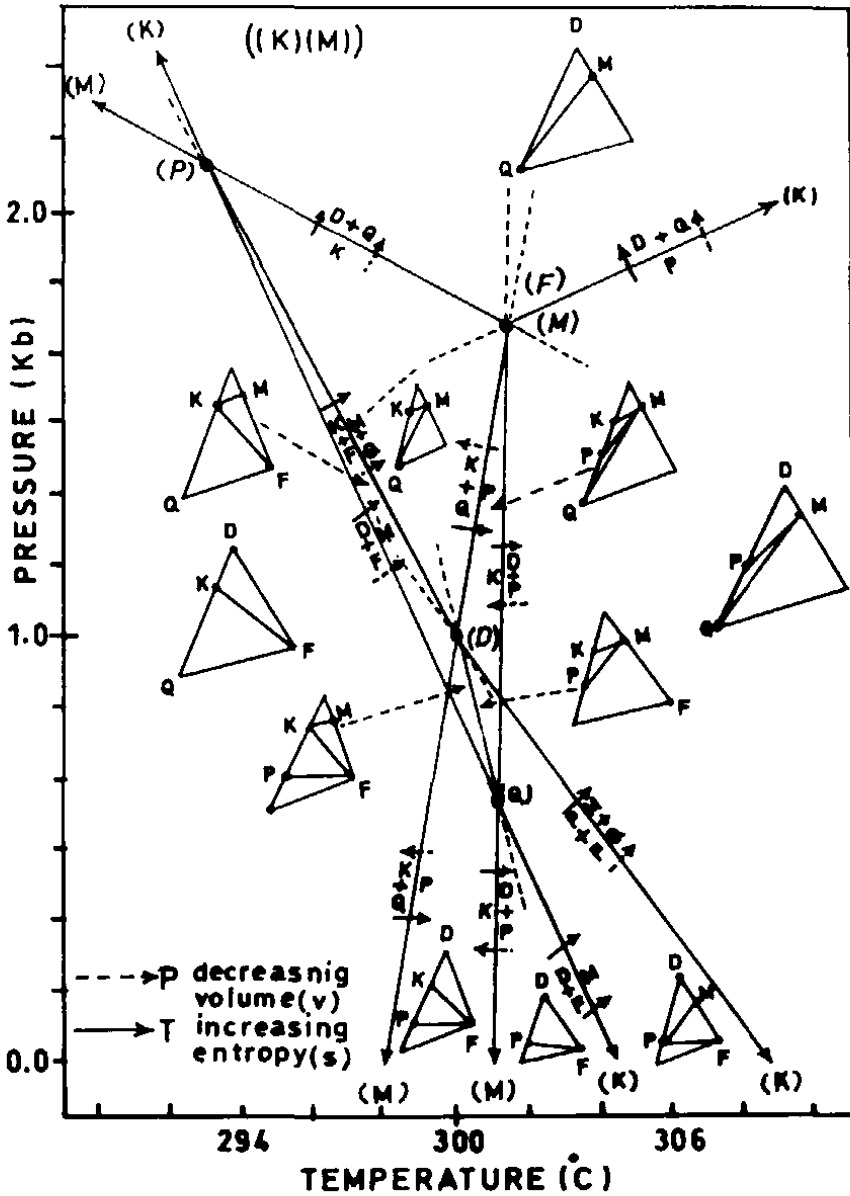
Fig. 7. Topology of the oriented partially-closed net of maximum closure in the system KASH [net ((K) (M)) of Fig. 6g].

(M)), but would change the application of the P-T diagram to natural environments. By contrast, a change in the volume sign would cause pyrophyllite to be stable on the high pressure side of the univariant line and the net (Fig. 7) would become impossible to orient with respect to the P axis. It is to be noted that the stable assemblage diaspore-quartz-pyrophyllite is rarely, if ever, reported from natural systems.

Reaction (D,F,M): K + 2 Q = P + W has been experimentally studied by [16] who reported equilibrium conditions of this reaction at P fluid = P total of : 325° +

20°C at 1 Kbar, 345° + 10°C at 2 Kbar, and 375° + 15°C at 4 Kbar. Reed and Hemley [17] previously placed the upper stability limit for K + Q at 300°C and 1 Kbar

Winkler [18] has discussed the stability limits of pyrophyllite and concluded that this mineral may form in the very low grade of metamorphism in pelitic rocks (prehnite-pumpelyite-chlorite zone). In his thermodynamic model of some equilibria in the system alumina-silica-water [5] indicates that pyrophyllite is stable during very low-grade metamorphism of sedimentary rocks. This would imply that pyrophyllite can form in natural systems almost at the beginning of metamorphism. He also suggests that the lower stability limits of pyrophyllite may extend to very low temperatures such as these prevailing under diagenetic conditions. The results of [16] would place the lower limit of pyrophyllite stability in the low grade metamorphic field (lower limit of the greenschist facies). According to both [18] and [5,19] the equilibrium temperature of the reaction was over estimated.

It should be noted that [5,18, p.334] suggest that the upper stability limit of pyrophyllite is bound by the equilibrium reaction $P = Q + Al_2SiO_5 + W$, which may occur at 400°C and 1 Kbar, or 430°C and 3.9 Kbar. This suggests that andalusite and kyanite can form in the greenschist facies of metapelites [18, p.334].

To confirm or reject the above mentioned propositions a temperature-pressure traverse across the univariant line (D,F,M) was made by running SUPCRT (a computer program run by the geochemistry group in Indiana University) for the reaction K + 2Q = P + W. The data obtained (Table 4) were used to compute the thermodynamic properties associated with the reaction and to determine the sign and magnitude of slope for the univariant curve (D,F,M) according to the following steps:

First, log Kp (equilibrium constant) is used to calculate the fugacity of water (fH_2O) under which kaolinite, pyrophyllite, and quartz coexist at equilibrium:

$$Kp = \frac{a_P \cdot fH_2O}{a_K \cdot a_Q}$$

Considering the three solid species (P,K and Q) as pure phases their activities (a) would be unity and, therefore:

$$Kp = fH_2O, \quad \text{that is, } \log fH_2O = \log Kp$$

From log Kp given in Table 4, fH_2O is calculated.

Second, the fugacity coefficients were used to calculate the fugacity of pure water ($f° H_2O$) at the T and P of interest.

Table 4. Equilibrium constant (Kp) and calculated water fugacities and activities between 1 bar and 5001 bars pressure and 0 to 810°C temperature for the reaction (D,F,M) : K + 2Q = P + W (SUPCRT data).

P (Bar)	T (Deg C)	Equilibrium Constant Kp (T,P)	Fugacity of water (fH$_2$O)	Fugacity coeffic. of water	Fugacity pure water (f°H$_2$O)	Activity of water (aH$_2$O)
1.000	00.0	− 4.09914	0.00008	0.006111	0.00611	0.0131
	30.0	− 2.95928	0.00110	0.042430	0.04243	0.0259
	90.0	− 1.24299	0.05715	0.69330	0.69330	0.0824
	150.0	− 0.02586	0.94219	0.99150	0.99150	0.9503
	210.0	+ 0.87098	7.42285	0.99550	0.99550	7.4634
	270.0	+ 1.55108	35.5697	0.99700	0.99700	35.677
	330.0	+ 2.07829	19.7540	0.99790	0.99790	120.01
	390.0	+ 2.49400	311.889	0.99860	0.99860	312.33
	450.0	+ 2.82616	670.132	0.99910	0.99910	670.74
	510.0	+ 3.09426	1242.40	0.99930	0.99930	1242.3
	570.0	+ 3.31231	2052.63	1.00000	1.00000	2052.6
	630.0	+ 3.48308	3041.45	1.00000	1.00000	3041.5
	690.0	+ 3.62585	4225.23	1.00000	1.00000	4225.2
	750.0	+ 3.74689	5583.29	1.00000	1.00000	5583.3
	810.0	+ 3.85066	7090.23	1.00000	1.00000	7090.2
1001	00.0	− 3.75137	0.00018	0.000013	0.01301	0.0136
	30.0	− 2.64467	0.00227	0.000086	0.08609	0.0263
	90.0	− 0.98270	0.10406	0.001268	1.26927	0.0820
	150.0	+ 0.20312	1.59632	0.007831	7.83883	0.2036
	210.0	+ 1.07311	11.8834	0.02836	28.3884	0.4168
	270.0	+ 1.73228	53.9859	0.07229	72.3623	0.7461
	330.0	+ 2.24273	174.876	0.14480	144.945	1.2065
	390.0	+ 2.64471	441.276	0.24360	243.844	1.8097
	450.0	+ 2.96541	923.423	0.35930	359.659	2.5676
	510.0	+ 3.22382	1674.25	0.47810	478.578	3.4984
	570.0	+ 3.43355	2713.68	0.58750	588.088	4.6143
	630.0	+ 3.60083	0.67910	679.779	679.779	5.8676
	690.0	+ 3.73627	5448.41	0.75250	753.253	7.2332
	750.0	+ 3.85092	7094.47	0.81020	811.010	8.7477
	810.0	+ 3.94885	8888.94	0.85530	856.155	10.382
2001	00.0	− 3.40554	0.00039	0.00014	0.02801	0.0140
	30.0	− 2.33178	0.00466	0.00085	0.17009	0.0274
	90.0	− 0.71492	0.19279	0.00137	2.27514	0.0847
	150.0	+ 0.43098	2.69762	0.006596	13.1986	0.2044
	210.0	+ 1.27428	8.8053	0.02292	45.8629	0.4100

Table 4. Continued.

P (Bar)	T (Deg C)	Equilibrium Constant Kp(T,P)	Fugacity of water (fH₂O)	Fugacity coeffic. of water	Fugacity pure water (f°H₂O)	Activity of water (aH₂O)
	270.0	+ 1.91267	81.7843	0.05682	113.697	0.7193
	330.0	+ 2.40647	254.959	0.11190	223.912	1.1387
	390.0	+ 2.79481	623.462	0.18740	374.987	1.6629
	450.0	+ 3.10414	1270.98	0.27810	556.478	2.2840
	510.0	+ 3.35291	2253.77	0.37740	755.177	2.9844
	570.0	+ 3.55439	3584.18	0.47800	956.478	3.4773
	630.0	+ 3.71859	5231.06	0.57330	1147.17	4.5600
	690.0	+ 3.84669	7025.71	0.65950	1319.66	5.3239
	750.0	+ 3.95487	9013.01	0.73490	1470.54	6.1219
	810.0	+ 4.04704	11144.0	0.79880	1598.40	6.9720
3001.	00.0	− 3.06163	0.00087	0.000019	0.05702	0.0152
	30.0	− 2.02059	0.00954	0.000159	0.32711	0.0292
	90.0	− 0.45296	0.35241	0.001337	4.01234	0.0878
	150.0	+ 0.65769	4.54669	0.007276	21.8353	0.2082
	210.0	+ 1.47449	29.8188	0.02421	72.6542	0.4104
	270.0	+ 2.09223	123.660	0.05821	174.688	0.7079
	330.0	+ 2.56949	371.009	0.11220	336.712	1.1021
	390.0	+ 2.94429	879.610	0.18520	555.785	1.5826
	450.0	+ 3.24232	1747.11	0.27270	818.373	2.1349
	510.0	+ 3.48153	3030.61	0.36900	1107.37	2.7368
	570.0	+ 3.67480	4729.33	0.46830	1405.37	3.3652
	630.0	+ 3.83241	6789.54	0.56450	1694.07	4.0131
	690.0	+ 3.95711	9059.62	0.65420	1963.25	4.6146
	750.0	+ 4.05881	11450.1	0.73520	2206.34	5.1896
	810.0	+ 4.14522	13970.8	0.80650	2420.31	5.7723
4001	00.0	− 2.71965	0.00191	0.000029	0.11603	0.0164
	30.0	− 1.71111	0.01945	0.000156	0.62416	0.0312
	90.0	− 0.19236	0.64216	0.001744	6.97774	0.0920
	150.0	+ 0.88326	7.64293	0.008908	35.6409	0.2144
	210.0	+ 1.67373	47.1770	0.02834	113.388	0.4161
	270.0	+ 2.27097	186.625	0.06596	263.906	0.7072
	330.0	− 2.73180	539.262	0.12410	496.524	1.0861
	390.0	+ 3.09314	1239.20	0.20130	805.401	1.5386
	450.0	+ 3.37994	2398.50	0.29270	1171.09	2.0481
	510.0	+ 3.60965	4070.52	0.39290	1571.19	2.5907
	570.0	+ 3.79477	6234.05	0.49560	1982.90	3.1439
	630.0	+ 3.94531	8816.78	0.59560	2383.00	3.6999

Table 4. Continued.

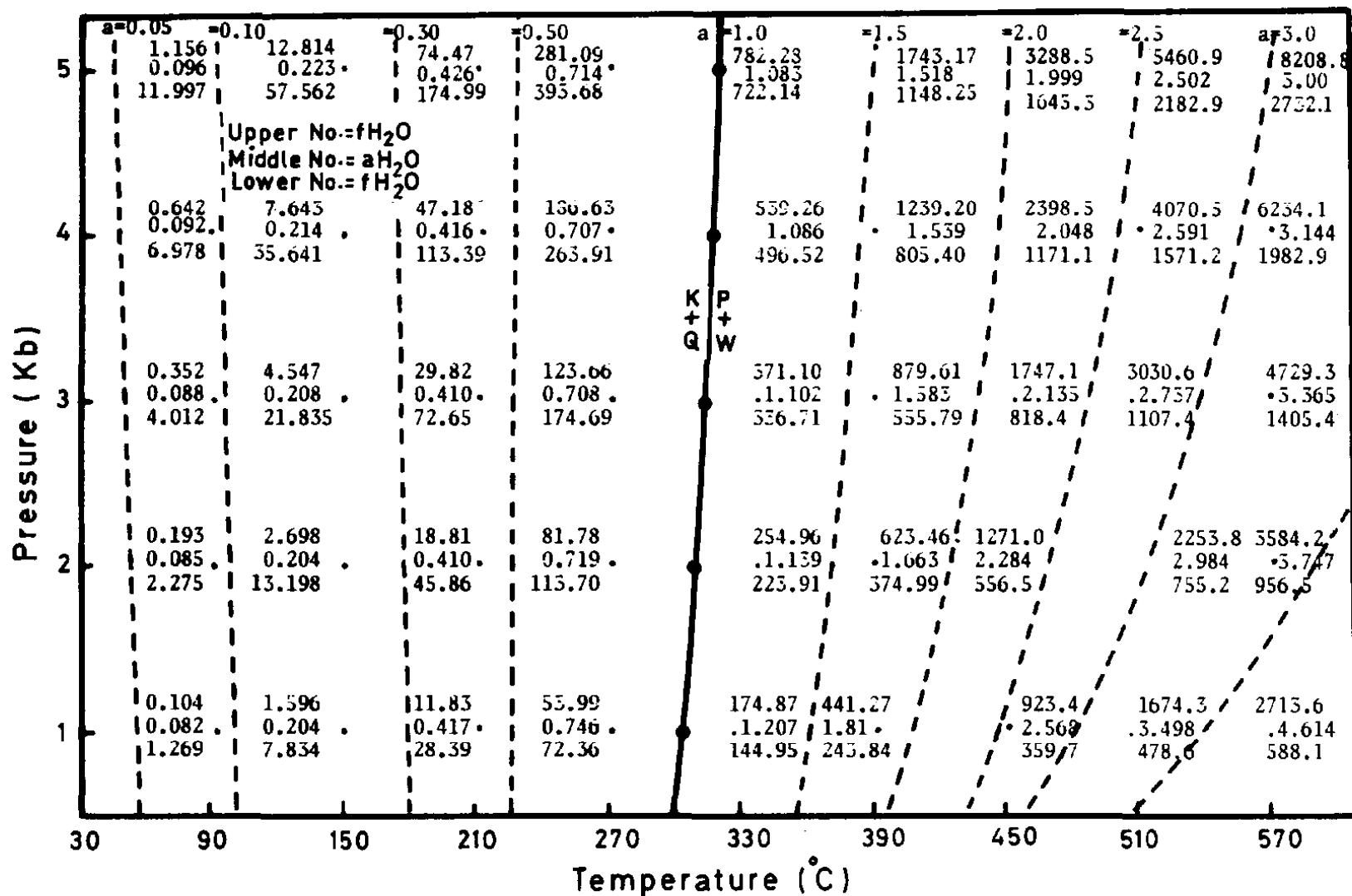| P (Bar)	T (Deg C)	Equilibrium Constant Kp(T,P)	Fugacity of water (fH$_2$O)	Fugacity coeffic. of water	Fugacity pure water (f°H$_2$O)	Activity of water (aH$_2$O)
	690.0	+ 4.06753	11682.3	0.68940	2758.29	4.2354
	570.0	+ 4.16276	14546.6	0.77490	3100.38	4.6919
	810.0	+ 4.24341	17515.0	0.85110	3405.25	5.1435
5001	00.0	− 2.37960	0.00417	0.000046	0.23005	0.0181
	30.0	− 1.40333	0.03951	0.000245	1.22525	0.0323
	90.0	+ 0.06294	1.15595	0.002399	11.9974	0.0964
	150.0	+ 1.10767	12.8136	0.011510	57.5615	0.2226
	210.0	+ 1.87199	74.4715	0.003499	174.985	0.4256
	270.0	+ 2.44885	281.093	0.07872	393.679	0.7140
	330.0	+ 2.89336	782.276	0.14440	722.144	1.0833
	390.0	+ 3.24134	1743.17	0.22960	1148.23	1.5181
	450.0	+ 3.51700	3288.52	0.32900	1645.33	1.9990
	510.0	+ 3.73726	5460.85	0.43650	2182.94	2.5016
	570.0	+ 3.94428	8208.81	0.54630	2732.05	3.0046
	630.0	+ 4.05780	11423.5	0.65230	3262.15	3.5018
	690.0	+ 4.17559	14982.7	0.75290	3765.25	3.9729
	750.0	+ 4.26670	18479.9	0.84190	4210.34	4.3892
	810.0	+ 4.34160	21958.4	0.92260	4613.92	4.7592

Third, using calculated fH$_2$O and f°H$_2$O at the T and P of interest, the activity of water (aH$_2$O) can be computed:

$$aH_2O = fH_2O / f° H_2O$$

Fourth, the T and P of interest (Table 4) are used to construct a P-T diagram for reaction (D,F,M) on which fH$_2$O, f° H$_2$O, and aH$_2$O were contoured (Figs. 8 and 9). Note that across the univariant lines in the two diagrams the reactants and products are at equilibrium when:

$$fH_2O = f° H_2O, \text{ that is, when } aH_2O = 1.0$$

Therefore, by locating on the diagram all such points, the T and P at which the reaction attains equilibrium conditions can be found, or the minimum T at which the low temperature assemblages react to yield high temperature phases at the pressure of interest can be determined. The results will help to define the slope of the uni-variant line.

Pressure (Kb)

| a=0.05 | =0.10 | =0.30 | =0.50 | a | =1.0 | =1.5 | =2.0 | =2.5 | a=3.0 |

5
1.156   12.814   74.47   281.09   782.23   1743.17   3288.5   5460.9   8208.8
0.096   0.223   0.426   0.714   1.083   1.518   1.999   2.502   5.00
11.997   57.562   174.99   393.68   722.14   1148.25   1645.3   2182.9   2732.1

Upper No.=fH$_2$O
Middle No.= aH$_2$O
Lower No.= f H$_2^0$O

4
0.642   7.643   47.18   130.63   539.26   1239.20   2398.5   4070.5   6254.1
0.092   0.214   0.416   0.707   1.086   1.539   2.048   2.591   3.144
6.978   35.641   113.39   263.91   496.52   805.40   1171.1   1571.2   1982.9

K   P
+   +
Q   W

3
0.352   4.547   29.82   123.66   571.10   879.61   1747.1   3030.6   4729.3
0.088   0.208   0.410   0.708   1.102   1.585   2.135   2.757   5.365
4.012   21.835   72.65   174.69   336.71   555.79   818.4   1107.4   1405.4

2
0.193   2.698   18.81   81.78   254.96   623.46   1271.0   2253.8   3584.2
0.085   0.204   0.410   0.719   1.139   1.663   2.284   2.984   5.747
2.275   13.198   45.86   113.70   223.91   374.99   556.5   755.2   956.5

1
0.104   1.596   11.83   55.99   174.87   441.27   923.4   1674.3   2715.6
0.082   0.204   0.417   0.746   1.207   1.81   2.568   3.498   4.614
1.269   7.834   28.39   72.36   144.95   243.84   359.7   478.6   588.1

Temperature (°C)

30   90   150   210   270   330   390   450   510   570

Fig. 8. P-T diagram for the reaction (D,F,M) in which aH$_2$O, fH$_2$O, and f°H$_2$O are contoured.
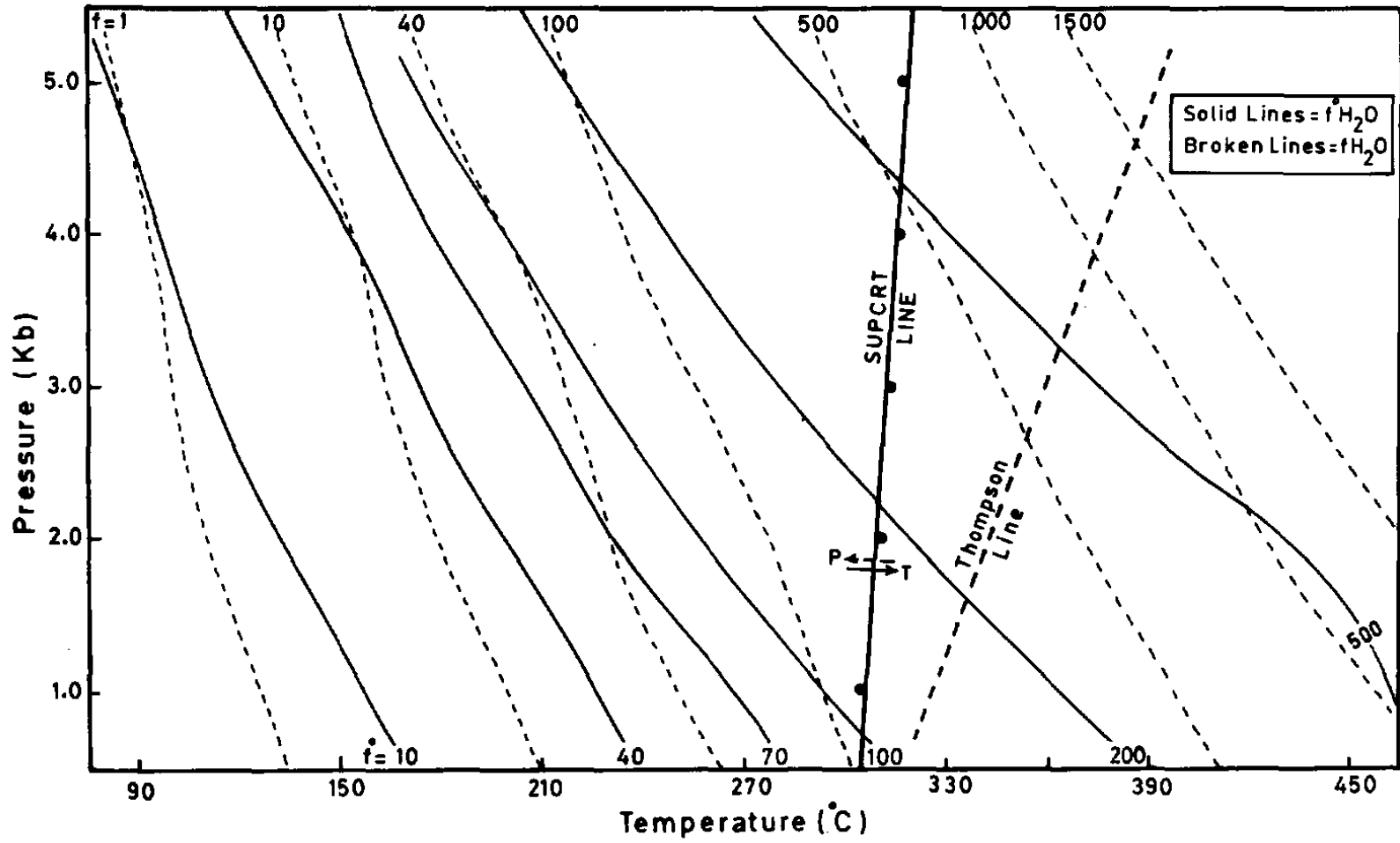
Fig. 9. P-T diagram, showing the SUPCRT line, Thompson line, and contours of fH₂O and f°H₂O.

For reaction (D,F,M): K + 2Q = P + W the diagrams (Figs. 8 and 9) reveal the following equilibrium conditions:

303°C at 1 Kbar
310°C at 2 Kbar
314°C at 3 Kbar
316°C at 4 Kbar
317°C at 5 Kbar

This shows that the univariant line generated by the reaction has a very steep positive slope and equilibrium T of about 312°C. The phases pyrophyllite and water are the high T and P assemblages. These results are lower than the experimental results of [16] but the slopes are in agreement as shown on Fig. 9. It should be noted, again, that uncertainities in both data sets caused the disagreement between the positions of the two univariant lines. Zen [14] has discussed this matter in detail and pointed out that the curves for dehydration reactions such as K + Q = P + W cannot be located precisely on a P-T net because of its high sensitivity to the aggregate uncertainities in thermochemical data. However, the phase diagram constructed here has undoubted use for geologic interpretation provided these limitations are taken into consideration. Furthermore, the difference in temperature does not affect the previous orientation of the P-T net. Therefore, the results obtained here are consistent with the data of [16] and it can be stated that Thompson does over estimate the equilibrium temperature of reaction (D,F,M).

Chemical Potential

Chemical potential gradient established by changes in P,T,aH_2O, and mineral assemblages can be shown on an activity diagram or a quantitative chemical potential diagram ($\mu - \mu$ diagram). Table 5 shows the stoichiometric coefficients of components (oxides + water) present in the system and the free energies of formation for the different phases taken from two sources of thermochemical data. A quantitative $\mu K_2O - \mu SiO_2$ diagram has been constructed (Fig. 10) assuming that μAl_2O_3 is constant. The data from [20] yield the diagram shown in heavy bold lines on Fig. 10 indicating stability fields of the different phases in the system. Diaspore is metastable with respect to gibbsite so in the presence of gibbsite the stability field of diaspore becomes restricted to a narrow region along a line called diaspore stability. Gibbsite is stable under high μAl_2O_3 but with increasing μSiO_2 kaolinite, then pyrophyllite become stable whereas with increasing μK_2O and μSiO_2 at constant μAl_2O_3 muscovite and microcline become the stable phases.

Table 5. Oxide formulae and molar free energies of formation of the different species at 298.15°C temperatures; (1) from [2] and (2) from [20].

Species	SiO$_2$	K$_2$O	Al$_2$O$_3$	H$_2$O	G° (Kcal) (1)	G° (Kacl) (2)
Quartz	1	0	0	0	$-$ 204.659	$-$ 204.646
Water	0	0	0	1	$-$ 56.678	$-$ 56.688
Potash	0	1	0	0	$-$ 76.981	$-$ 77.056
Alumina	0	0	1	0	$-$ 378.162	$-$ 374.824
Diaspore	0	0	1	1	$-$ 220.362	$-$ 218.402
Gibbsite	0	0	1	3	$-$ 276.025	$-$ 276.168
Pyrophyllite	4	0	1	1	$-$ 1259.413	$-$ 1255.977
Kaolinite	2	0	1	2	$-$ 908.070	$-$ 905.614
Microcline	6	1	1	0	$-$ 894.438	$-$ 895.374
Muscovite	6	1	3	2	$-$ 1238.592	$-$ 1336.301
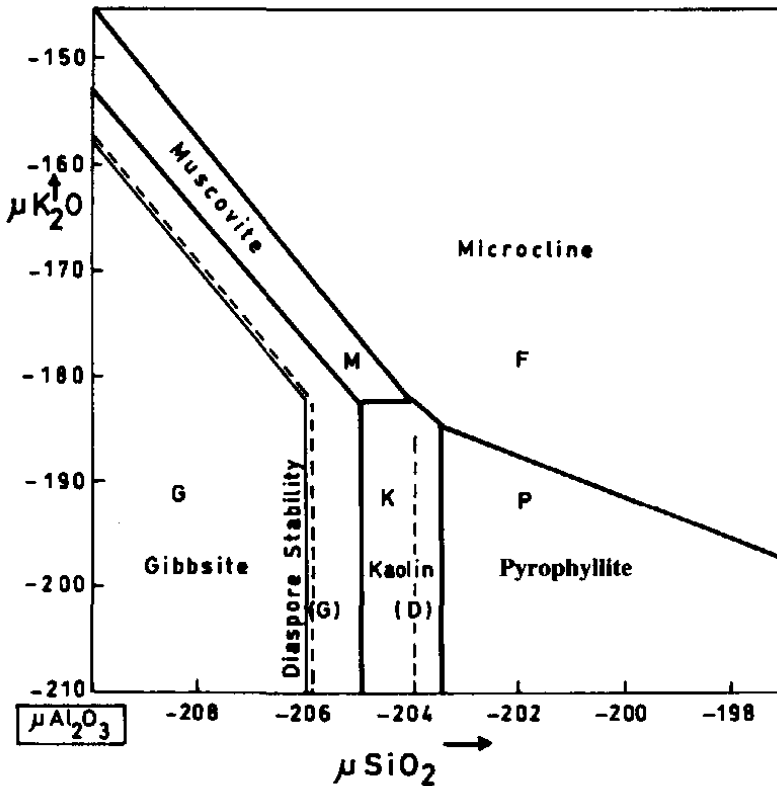
Fig. 10. Quantitative chemical potential diagram constructed using SUPCRT data (Table 5) and data from [2] (broken lines) at T = 278. 15°K.

Using data from [2], it is found that the diaspore-gibbsite relation is reversed so that diaspore becomes the stable aluminum hydrate (Fig. 10, dashed lines marked (D) and (G)). These controversial resutls show the effect of different, or erroneous, thermodynamic information on the interpretation of phase diagrams. It should be noted that the stability of gibbsite with respect to diaspore is in agreement with the activity-activity diagram of [21, p. 253].

Geologic Applications

The petrology and mineralogy of seven pyrophylite deposits in the volcanic slate belt of the Piedmont region, North Carolina were studied by [22]. Seven minerals found in these deposits belong to the system $K_2O–Al_2O_3–SiO_2–H_2O$. These include pyrophyllite, muscovite, kaolinite, andalusite, kyanite, diaspore, and quartz. Sykes, et al. [23] studied the pyrophyllite at Hillsborough, North Carolina and reported the minerals quartz, andalusite, topaz, sericite, pyrophyllite, and kaolinite. They observed the absence of diaspore from the paragenesis and concluded that the rocks did not contain enough Al_2O_3 to form diaspore as a separate phase. However, the following assemblages can tentatively be cited for the pyrophyllite in the metavolcanic slate belt of North Carolina : pyrophyllite-kaolinite-andalusite-quartz, pyrophyllite- kaolinite- quartz, pyrophyllite- diaspore- kaolinite, kaolinite-quartz-muscovite, pyrophyllite-kaolinite-muscovite, and pyrophyllite - quartz - muscovite. The assemblage pyrophyllite-kaolinite - quartz is evidence of the occurrence, in natural systems, of the equilibrium $K+2Q = P + W$. On the phase diagram, this reaction occurs at low P and high T and may indicate the lower stability limit of pyrophyllite (Fig. 7). This is in agreement with [5, 18, p. 334]. Zen [22] confirms that textural evidence suggested that this 3-phase assemblage represents an equilibrium assemblage. It is noticeable that [23] believe that the mineral parageneses and textures indicate disequilibrium assemblages for the Hillsborough pyrophyllite occurrence and that water, silica, and maybe alumina have behaved as mobile components during its formation. Kaolinite and pyrophyllite occur as intermixed phases. Also the assemblage pyrophyllite-diaspore-kaolinite is evidence for the occurrence in geological systems of the reactions $2D+P+2W = 2K$. On the phase diagram (Fig. 7), kaolinite is the lowest P phase and it decomposes to form pyrophyllite, diaspore, and water at low P and at T above that of the invariant point (Q). It may also be suggested that the previous association is good evidence of the natural occurrence of the equilibrium univariant relation $K = 2D + 2Q + W$. This is possible if it is assumed that quartz is a minor phase which is totally consumed by reversal of the process. Other natural occurrences are also available. In a study of petrographic relations in some bauxite and diaspore deposits from North Carolina and Georgia [24] discussed desilication as a mechanism of formatin for aluminium hydrates. Kaolinite forms first by weathering of potash feldspars. Then, by removal of silica from kaolinite, aluminium hydrates such as diaspore, gibbsite, and boehmite were formed. This

Jomaah A. Alawi

approach may confirm the occurrence of the equilibrium $K = 2D + 2Q$ which, in Fig. 7 occurs with increasing P and at T slightly higher than that of the invariant point (P).

Day [5] reported that Chennaux and Dunoyer de Segonzac observed in the Siluro-Devonian deposits from the Sahara the presence of detrital micas surrounded by rims of pyrophyllite. Similar rims of pyrophyllite also occur around kaolinite and detrital quartz in the same deposits. The association of alteration rims is unlikely to represent equilibrium assemblages but such assemblages as muscovite-pyrophyllite, kaolinite-pyrophyllite-quartz may confirm the natural occurrence of two of the reactions belonging to the system KASH. One of them is the reaction $K + 2Q = P + W$ discussed above. The second may be the reaction $M + 4Q = P + F$. However, on the P-T net ((K)(M)) the pair $P + F$ decomposes at increasing T and P to form muscovite and quartz. This constrains the stability of pyrophyllite and feldspar to the low P and T side of the univariant line (D,K) on the P-T spare (Fig. 7). These results are in agreement with the suggestion of [18] that pyrophyllite and potassium feldspar are an incompatible pair in slates and phylites so that when the two phases come into contact they react to form muscovite. The petrographic observations (the rocks described above) however, are in disagreement with the P-T net which suggests that $P + F$ could coexist stably at the low P and T side of the univariant line (D,K). Thus, it can be suggested that the pyrophyllite observed in the above cited natural assemblage (the saharian deposits) may be the product of K-leaching by pore fluids.

Note that the natural occurrences discussed above do not include any potash feldspars. Therefore, when potash feldspar is involved in one of the reactions used in the construction of the P-T diagram the equilibrium cannot be confirmed. Four such reactions contain K-feldspar, (D,Q), (D,P), (D,K) and (Q,P,K). In these reactions potash feldspar is incompatible with, kaolinite, pyrophyllite, or diaspore during metamorphism and it reacts with one of them to form muscovite. Either water, quartz, or both are present as distinct phases within these four systems.

Zen [22] has pointed out that the occurrence of the 3-phase assemblages, pyrophyllite-kaolinite-quartz, diaspore-pyrophyllite-kaolinite, and andalusite-quartz-pyrophyllite indicates that H_2O behaved as a buffered chemical component during the formation of pyrophyllite deposits of North Carolina. This excludes the presence of a free (unbuffered) solution phase suggested if these bodies were to be formed by hydrothermal replacement.

References

[1] Zen, E-An. "Construction of Pressure-Temerautre Diagrams for Multicomponent Systems After the Method of Schreinemarker – A Geometric Approach." *U.S.G.S., Bull.*, 1225 (1966), 1-56.

[2] Robie, R.A.; Hemingway, B.S., and Fisher, J.R. "Thermodynamic Properties of Minerals and Related Substances at 298.15°K and 1 bar (10 pascals) Pressure and at Higher Temperatures." *USGS, Bull.* 1452 (1978), 1-456.

[3] Zen E-An, and Roseboom, E.H. Jr. "Some Topological Relationships in Multisystems of n + 3-Phases, III: Ternary Systems." *Am J. Sci.*, 272 (1972), 677-710.

[4] Day, H.W. "Geometrical Analysis of Phase Equilibria in Ternary System of Six Phases." *Am. J. Sci.*, 272 (1972), 711-734.

[5] Day, H.W. "A Working Model of Some Equilibria in the System Alumina-Silica-Water." *Am. J. Sci.*, 276 (1976), 1254-1284.

[6] Burt, D.M. "Hydrolysis Equilibria in the System $K_2O-Al_2O_3 - SiO_2-H_2O - Cl_2O-1$, Comments on Topology." *Econ. Geol.*, 71 (1976), 665-671.

[7] Burt, D.M. "A Working Model of some Equilibria in the System Alumina-Silica-Water, Discussion." *Am. J. Sci.*, 278 (1978), 244-250,

[8] Anderson, G.M. "Error Propagation by the Monte Carlo Method in Geochemical Calculation, Geochim." *Cosmochim Acta,* 40 (1976), 1533-1538.

[9] Bird, G.W. and Anderson, G.M. "The Free Energy of Formation of Magnesian Cordierite and Phologobite." *Am. J. Sci.*, 273 (1973), 84-91.

[10] Gordon, T.M. "Determination of Internally Consistent Thermodynamic Data from Phase Equilibrium Experiments." *J. Geol.*, 81 (1973), 199-208.

[11] Kerrick, D.M., and Slaughter, J. "Comparison of Methods for Calculating and Extrapolating Equilibria in P-T-XCO2 Space." *Am. J. Sci.* 276 (1976), 883-916.

[12] Richardson, S.W., Gilbert, M.C., and Bell, P.M. "Experimental Determination of Kyanite-Andalusite and Andalusite-Sillimanite Equilibria; the Aluminum Silicate Triple Point." *Am. J. Sci.*, 267 (1969), 259-272.

[13] Zen, E-An. "Gibbs Free Energy, Enthalpy, and Entropy of Ten Rock Forming Minerals: Calculations, Discrepancies, Implications." *Am. Mineral.*, 57 (1972), 524-553.

[14] Zen, E-An. "The Phase-Equilibrium Calorimeter, the Petrogenetic Grid, and a Tyranny of Numbers." *Am. Mineral.*, 62 (1977), 189-204.

[15] Ulbrich, H.H. and Merino, E "An Examination of Standard Enthalpies of Formation of Selected Minerals in the System $SiO_2-Al_2O_3-Na_2O - K_2O - H_2O$." *Am. J. Sci.*, 274 (1974), 510-542.

[16] Thompson, A.B. "A Note on the Kaolinite-Pyrophyllite Equilibrium." *Am. J. Sci.*, 268 (1970), 454-458.

[17] Reed, B.L., and Hemley, J.J. "Occurrence of Pyrophylite in the Kekiktuk Conglomerate, Brooks Range, North Eastern Alasca." *U.S.G.S. Prof. Pap.*, 550C (1966), 162-166.

[18] Winkler, H.G.F. "Petrogenesis of Metamorphic Rocks, 4th ed., New York: Springer-Verlag, Inc., 1976.

[19] Day, H.W. "A Working Model of some Equilibria in the System Alumina-Silica-Water, Reply." *Am. J. Sci.*, 278 (1978), 250-253.

[20] Helgeson, H.C., Delany, J.M., Nesbitt, H.W., and Bird, D.K. "Summary and Critique of the Thermodynamic Properties of Rock-Forming Minerals. *Am. J. Sci.*, 278 (1978),

[21] Helgeson, H.C., Brown, T.H., and Leeper, R.H. *Handbook of Theoretical Activity Diagrams Depecting Chemical Equilibria in Geologic Systems Involving an Aqueous Phase at One Atm and $O°$ to 300°C.* San Francisco: Freeman, Cooper, and Company, 1969.

[22] Zen, E-An. "Mineralogy and Petrology of the System $Al_2O_3 - SiO_2 - H_2O$ in some Pyrophyllite Deposits of North Carolina." *Am. Mineral.*, 46 (1961), 52-66.

[23] Sykes, M.L., and Moody, J.B. "Pyrophyllite and Metamorphism in the Carolina Slate Belt." *Am Mineral.*, 63 (1978), 96-108.

[24] Allen, V.T. "Petrographic Relations in Some Typical Bauxite and Diaspore Deposits." *Geol. Soc. Am., Bull.*, 63 (1952), 649-688.

توازن الأصناف في النظام المكون من البوتاس ـ الألومينا ـ السليكا ـ الماء

جمعـة بن عبدالرحيـم عوض العلاوي

قسم الجيولوجيا ـ كلية العلوم ـ جامعة الملك سعود ـ ص . ب ٢٤٥٥ ـ الرياض ١١٤٥١ ـ

المملكة العربية السعودية

(أُستلم في ٢٧ شعبان ١٤٠٩هـ، قُبل للنشر في ٢٠ شوال ١٤١٠هـ)

ملخص البحث . لقد اختيرت ستة أصناف صلبة وهي الدياسبور، والميكروكلين والكوارتز والبيروفيلليت والكاولينايت والمسكوفيت لرسم شبكة ضغطية حرارية (شبكة P-T) للنظام المكون من البوتاس ـ الألومينا ـ السيليكا ـ الماء ($K_2O-Al_2O_3-SiO_2-H_2O$) . هذا النظام المتعدد ذو الثلاث مركبات والسبعة أصناف يحتـوي على ست نقط غير قابلة للتغير، وخمسة عشر منحنى أحادي التغير وهي عند توصيلها ببعضها البعض تصنع شبكة ضغطية حرارية فريده وباستخدام المعطيات الثرموديناميكية والبناء الهندسي والتحليل البياني حسب قاعدة شراين ميكر يمكن رسم عشر شبكات ضغطية حرارية ثم بالاعتماد على إشارة الانتروبي ومقدارها وأيضًا على الأحجام الجزيئية وميول المنحنيات المصاحبة للتفاعلات أحادية التغير يمكن توجيه جميع الشبكات بالنسبة لاحداثيات درجة الحرارة والضغط وقد وجد أنه لا يوجد سوى شبكة واحـدة فقط مناسبـة لتمثيل العلاقات بين الأصناف ضمن النظام المدروس وهي شبكة ((كاولينايت) (مسكوفيت)) أي ((M) (K)). وقد وجد كذلك بأنه عند استخدام معطيات ثرموديناميكية من مصادر مختلفة يتغير توجيه الشبكة وتختلف النتائج مما يدعو إلى الشك في مصداقية استخدام المعطيات الثرموديناميكية عند الاختيار بين الأشكال البيانية الممكنة وإلى عدم القدرة على التأكد من صلاحية الشبكة التي وقع عليها الاختيار لذا فقد استخدم برنامج خاص بالحاسب الآلي (SUPCRT) لدراسة التفاعل دياسبور + كوارتز = بيروفيلليت + ماء تحت ظروف مختلفة عديدة من الضغط ودرجة الحرارة ثم استخدمت المعلومات الناتجة لحساب ضغط ودرجة حرارة التوازن الكيميائي ولتحديد إشارة ميل الخط أحادي التغير ومقدار هذا الميل لتأكد مصداقية التوجيه المقترح للشبكة وقد أعطت النتائج ميل موجب شديد الانحدار ودرجـة حرارة إتزان مقدارها ٣١٢°م عند ضغط = ٢٫٥ كيلوبار. كذلك لقد عمل رسم بياني للجهد الكيميائي (SiO_2 µ - K_2O µ) باستخدام مصدرين ثرموديناميكيين مختلفين وقد عززت نتائج الرسم مدى تأثير عامل الخطأ في معطيات الثرموديناميكية على تفسير علاقات الأصناف .

وبـالتـطبيق على الموجـودات الجيولـوجية الطبيعية خاصة على رواسب الطين المتحولة ورواسب البيروفيلليت تبين أن الرسم البياني للأصناف الذي حصل عليه ـ أي الشبكة ((M) (K)) ـ يمكن أن يحدد العلاقات المعدنية والتوازن الكيميائي في العمليات الطبيعية .